Accepted at Phys. Rev. B

-

Level statistics and Anderson delocalization in two-dimensional granular materials

Ling Zhang[1,2]†, Yinqiao Wang[2]†, Jie Zheng[2], Aile Sun[2], Xulai Sun[2], Yujie Wang[2], Walter Schirmacher[3], and Jie Zhang[2,4,*]
[1]*School of Automation, Central South University, Changsha 410083, China.*
[2]*School of Physics and Astronomy, Shanghai Jiao Tong University, Shanghai 200240, China*
[3]*Institut für Physik, Universität Mainz, Staudinger Weg 7, D-55099 Mainz, Germany and*
[4]*Institute of Natural Sciences, Shanghai Jiao Tong University, Shanghai 200240, China*
(Dated: March 2, 2021)

Contrary to the prediction of one-parameter scaling theory, that all waves in two-dimensional disordered materials are localized, Anderson localization is observed only for sufficiently high frequencies in an isotropically jammed two-dimensional disordered granular packing of photoelastic disks. More specifically, we have performed an experiment in analyzing the level statistics of normal-mode vibrations. We find that the level-distance distribution obeys Gaussian-Orthogonal-Ensemble (GOE) statistics of the Wigner-Dyson classification, in the low-frequency (boson-peak) and intermediate frequency regime, whereas in the high-frequency regime Poisson statistics is observed. This means that at the low and intermediate frequencies we have delocalized modes, and only at the very high frequencies localized modes exist. Evaluating the system-size dependence of the delocalization-localization crossover frequency we obtain evidence for a true transition with a mobility edge at 80 % of the Debye frequency and a value of the critical correlation-length exponent $\nu \sim 1.66$ being similar to that of the three-dimensional electronic Anderson model. We argue that for force-constant disorder one-parameter scaling might not be applicable.

PACS numbers: 83.80.Fg, 45.70.-n, 81.05.Rm, 61.43.-j
Keywords: level distance, boson peak, Anderson localization

Wave localization in amorphous materials has become one of the most spectacular phenomena in the field of condensed-matter physics since it was proposed by Anderson to describe the localization of electron waves[1,2]. With the continuous experimental advancement, Anderson localization has been found ubiquitously, such as the localization of ultra-cold atoms[3–6] and light and sound[7–10]. One commonly accepted view is that Anderson localization depends on dimension: waves are in general localized in one and two dimensions[2,11,12], including acoustic waves[13–15]. A mobility edge separating localized from extended waves is expected only in three dimensions. It has, however, been pointed out[13,15,16] that for weak disorder the localization length may become macroscopically large.

A number of studies[17–19] tried to relate Anderson localization to anomalous vibrational properties of phonons in glasses, in particular the so-called boson peak, which is an enhancement of the vibrational density of states, compared with Debye's ω^2 law[20–39]. Skepticism about this interpretation has been raised in later theoretical and numerical studies in three-dimensional systems[22,40,41], which point out that the boson peak and Anderson localization are two separate identities, obeying different statistics. Moreover, the boson peak is a universal characteristic of amorphous materials, independent of the actual dimensionality as observed in numerical[27,28,31,42–45] and experimental[37,38,46] studies of two-dimensional systems. Therefore, the situation is not clear. One essential scientific question is whether the vibrational properties of phonons in disordered systems are truly localized in two dimensions as commonly believed[13,14]. This is the main focus of the present work.

To address the above important question, we analyze the level statistics, which is extremely powerful in distinguishing the regime of Anderson localization from the delocalized one[47]. Schirmacher et al[22] found in a model calculation of a cubic lattice with disordered nearest-leighbor force constants that the level distances obey Gaussian-Orthogonal-Ensemble (GOE) statistics in the boson-peak regime and Poisson statistics only near the upper band edge, well above the boson-peak regime. They concluded, in accord with earlier work[48], that the modes around the boson peak are delocalized and localized states exist only at high frequencies. Recently it was discovered that a lattice of coupled masses and springs with random values[49,50] and truncated Lennard-Jones fluid[51] exhibit Anderson universality of disordered phonons, which means that the localization transition is in the same universality class as the electronic Anderson model. In both investigations the localization frequency is located near the upper band edge.

In recent years, Zhang et al[37] and Wang et al[38] have successfully used isotropically jammed disordered macroscopic packings of photoelastic disks to perform experimental studies of vibrations in disordered systems and in particular the nature of the boson peak. In these studies[37,38], the dynamical matrix, and hence the harmonic vibrational spectrum, can be directly constructed from the experimental measurements of the particle positions and the contact forces between the particles.

In this paper, we analyze the level-distance statistics of the vibrational normal modes of a two-dimensional isotropically jammed disk packing. We identify a localization-delocalization crossover slightly below the Debye frequency ω_D[52]. By performing a system-size analysis of the crossover

frequency and comparing the results corresponding to the prediction of the conventional theory for two-dimensional acoustic waves, based on the one-parameter scaling concept[13,15], we obtain unphysical results. However, the data can be well explained by a true delocaization-localization transition at 80 % of the Debye frequency with a correlation-length exponent ~ 1.66, which is similar to that of the three-dimensional electronic Anderson transition. These findings are paralleled with the case of electrons in the presence of disorder in the hopping integral (off-diagonal disorder)[53–55], where also a true transition is found in two dimension.

We prepared disordered isotropically jammed granular packings using a biaxial apparatus, which consists of a square frame of four mobile walls mounted on a powder-lubricated glass plate. Right under the plate, there is a circular polarizer sheet, below which a uniform LED light source is mounted. A high-resolution camera is placed two meters above the center of the biaxial apparatus, and a mobile circular polarizer sheet is placed right below the camera which records images of particle configurations and stresses. In order to maximize the degree of disorder we filled the square frame randomly with a 50%-50% bi-disperse mixture of $N = 2500$ photoelastic disks of sizes of $D = 1.4$ cm and $D = 1.0$ cm. First, we prepared a random packing slightly below the jamming point[37,38]. Next, we applied an isotropic compression to the random initial packing until its packing fraction reached the jamming point $\sim 84\%$. At this point, we applied a homogeneous tapping to create an isotropic and stress-free packing[56]. Then, we continued to compress the system quasi-statically and isotropically to prepare jammed packings at different pressure.

We emphasize that our jammed system consists of rather hard discs in comparison with the harmonic and Hertzian model systems studied numerically in the jamming literature[42,57], and that we are not near the isostatic (marginally stable) limit, but, instead, in the strongly jammed regime[58].

In order to establish the Hessian matrix $\mathcal{H}_{ij}$ we performed an accurate measurement of disk positions and interaction forces between disks, we then applied the pre-calibrated curves of contact forces (i.e., the normal and tangential components) versus deformation and determined the spring constants at each contact point. Finally, we mapped the isotropically jammed disk packing to a disordered network of coupled masses and springs, which is similar to the coupled harmonic oscillators of random spring constants except for the disordered network structure[22,49]. It is important to note that we are not probing our system dynamically[59]. We only use it to extract the forces between the disks, in order to obtain the Hessian matrix. Therefore, as our system is completely at rest, in our investigation any possible friction forces do not play a role.

The Hessian matrix $\mathcal{H}_{ij}$ is constructed following a standard procedure[37,38,60–62], whose eigenvalues are $\lambda = \omega^2$, with ω being the angular frequencies. Using the eigenvalue spectrum we are able to decide, whether or not the eigenstates of a certain spectral region are localized or not, i.e., whether the modal wave functions are confined to a certain spatial region of size ξ, where ξ is the localization length. In a quenched-

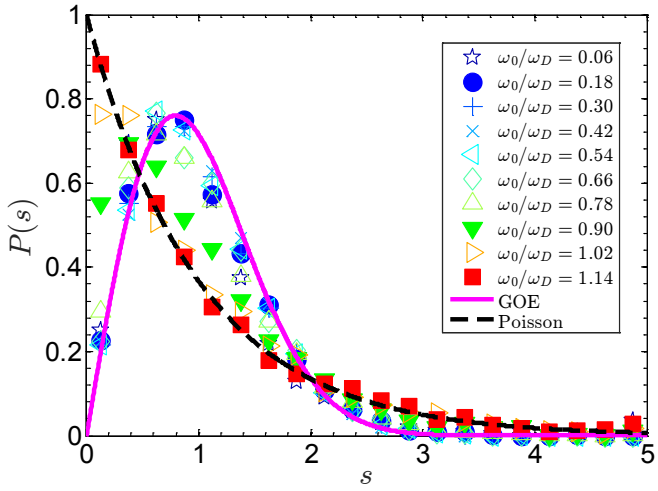

FIG. 1: Statistical distributions $P(s)$ of the normalized level distances s for 10 equal-frequency intevals around midpoints ω_0 of width $\Delta\omega/\omega_D = 0.12$, where ω_D is the Debye frequency[52], together with the GOE and Poissonian laws.

disordered material the eigenvalues corresponding to delocalized vibrational states cannot exhibit degeneracies (coinciding eigenvalues) due to the absence of spatial symmetries. This means that small distances between eigenvalues are strongly suppressed ("level repulsion"). On the other hand, if the states are localized, the wavefunction of different states mostly do not overlap, so they "do not know of each other", and accidental degeneracies may occur.

The presence or absence of level repulsion can be quantified using the universal statistics of random-matrix ensembles[47,63,64]. In order to compare with such universal spectra, the actual spectrum, corresponding to a certain level density $g(\lambda)$ must be unfolded to correspond to a constant level density $g(\epsilon) = const.$[22,41,51,51,65–70]. Here the eigenvalues ("levels") are the square of the eigenfrequencies $\lambda_i = \omega_i^2$, and we have $g(\omega) = 2\omega g(\lambda)$.

This unfolding procedure proceeds as follows: From the cumulative distribution function $F(\lambda) = \int_0^\lambda d\tilde{\lambda} g(\tilde{\lambda}) = \int_0^{\sqrt{\lambda}} d\omega\, g(\omega)$ a smoothed function $\widetilde{F}(\lambda)$ is calculated. We found that for all our data the function $\widetilde{F}(\lambda) = 1 - \exp\{-A\lambda^2 - B\lambda\}$ (with $A = 0.02\omega_D^{-4}$ and $B = \omega_D^{-2}$, $\omega_D =$ Debye frequency[52]) gives a good fit to the smoothed cumulative distribution function. The unfolded levels are then obtained as $\epsilon_i = \widetilde{F}(\lambda_i)$. In order to obtain the universal distance fluctuations, *normalized level distances* are defined as $s_i = |\epsilon_i - \epsilon_{i-1}|/\langle\Delta\epsilon\rangle$, where the mean level distance $\langle\Delta\epsilon\rangle$ equals the inverse of the number N_λ of levels.

Now, for *delocalized* states (level repulsion) one expects a universal level-distance distribution according to the Gaussian-orthogonal ensemble (GOE) of the Wigner-Dyson classification scheme[63,64]

$$P(s) = \tfrac{\pi}{2} s\, e^{-\frac{\pi}{2}s^2}. \qquad (1)$$

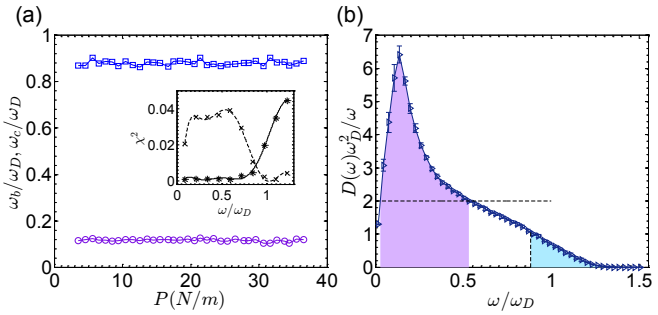

FIG. 2: (a) Main panel: The boson-peak position ω_b/ω_D (purple circles) and the ω_c/ω_D (blue squares) versus pressure p, in which the results have been ensemble averaged over 10 realizations, and the error bars are within symbol sizes. Inset: Chi-squared χ^2 of the level-distance statistics fitted by two distributions of (1) GOE (asterisks) and (2) Poisson (crosses) versus the ω/ω_D. The two lines are smoothed curves to locate the critical point ω_c/ω_D as their crossing point, which shows $\omega/\omega_D \approx 0.88$ at pressure $p = 26.5$ N/m.
(b) Reduced density of states $g_\omega(\omega)/\omega$, re-scaled by the Debye frequency ω_D at a typical value of pressure $p = 26.5$ N/m. Here the lavender area denotes the boson-peak region, and the light blue denotes the Anderson-localization regime. The horizontal dashed line denotes Debye*s density of states $g_D(\omega)/\omega = 2/\omega_D^2$, the vertical dashed line) the crossover frequency ω_c/ω_D.

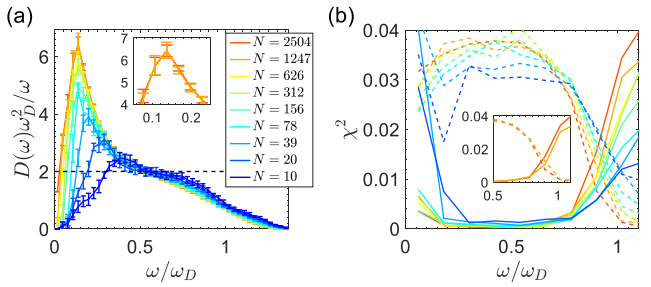

FIG. 3: (a) Reduced density of states $g_\omega(\omega)/\omega$ against ω/ω_D of different system sizes at a typical value of pressure $p = 26.5$ N/m. The horizontal dashed line represents the Debye model. Inset: Amplified boson-peak regime of the two largest sizes. (b) Chi-squares χ^2 vs the ω/ω_D for different system sizes at a typical value of pressure $p = 26.5$ N/m. Here, solid lines represent the χ^2 of GOE, while dashed lines are the χ^2 of poisson distributions. Different colors indicate different sizes as defined in (a). Inset: Amplified χ^2 curves of the two largest sizes. Note that results of a given size N are ensemble averaged over $\sim \frac{2500}{N} \times 9$ realizations.

On the other hand, for *localized* states (no level repulsion) one exprects a completely random , i.e. a Poissonian distribution

$$P(s) = e^{-s}. \tag{2}$$

In Fig. 1 we present the results of the level distance statistics of 9 independent realizations of disk arrangements at pressure $p = 26.5$ N/m. The results of other pressures are similar, and the error bars are within the symbol sizes. We have taken the statistics for intervals $\Delta\omega = 0.12\omega_D$ (where ω_D is the Debye frequency[52]) around midpoints covering the frequency range of the spectrum. We observe GOE statistics in the entire frequency range below a crossover frequency ω_c, which is slightly below the Debye frequency. Above ω_c we observe Poisson statistics, indicating localized states.

To identify the crossover frequency ω_c, we quantitatively characterize deviations between data points and fitting curves using GOE and Poisson statistics by calculating the χ^2 as a function of ω, as shown in the inset of Fig. 2(a). Here, the $\chi^2 = \sum(\tilde{y}_i - y_i)^2$, in which $\tilde{y}_i$ are the fitting values, and y_i are the original data points. From the inset of Fig. 2(a), we see that when $\omega_0/\omega_D < \omega_c/\omega_D$, the distributions are better described by GOE statistics, while in the regime of $\omega_0/\omega_D \geq \omega_c/\omega_D$, distributions are better described by Poisson statistics. The crossover point occurs around $\omega_c/\omega_D = 0.88 \pm 0.03$, which is nearly independent of pressure, as shown in the main panel (square symbols) of Fig. 2(a).

We have done a systematic analysis of the finite-size effect on the boson peak and the crossover frequency ω_c by changing the square of the system size N (we measure lengths from now on in units of the average particle diameter $\langle D \rangle$) from $N = 10$ up to $N = 2504$. The boson-peak position ω_b/ω_D decreases when N increases from $N = 10$ up to $N = 78$ and it quickly stabilizes to $\omega_b/\omega_D \approx 0.13$ when $N \geq 156$, as shown in Fig. 3(a). In addition, the upper limit of the boson-peak regime (i.e., the maximum frequency in the lavender color area of the boson peak regime) is a constant, nearly independent of N, as shown in Fig. 3(a). Moreover, shapes of the boson peak cease changing when $N \geq 1247$ so that the lower limit of the boson-peak regime and the boson-peak height stabilize, as shown in Fig. 3(a). The stabilization of the boson-peak shape profile can be better viewed in the inset of Fig. 3(a), where the profiles of $N = 1247$ and $N = 2504$ collapse on top of each other. When the boson peak evolves with N, the Anderson-localization regime in the density of states also evolves, but its profile shape shows very little change as N increases, as shown in Fig. 3(a).

We turn now to the evaluation of the crossover frequency ω_c with respect to the system size $N^{1/2}$. According to the scaling theory of wave localization[2,11] (as well as the self-consistent diagrammatic theory[12,71–73] and the generalized nonlinear sigma model[10,13,74–76]) in two dimensions the localization length in terms of the mean-free path $\ell(\omega)$ is given by

$$\xi(\omega) = \ell(\omega)\, e^{C\, k(\omega)\ell(\omega)}, \tag{3}$$

where $k = v\omega$ and v is the wave velocity and C a constant of order unity. On the other hand, the mean-free path for scattering of longitudinal (L) and transverse (T) waves is related to the corresponding sound velocities $v_{L,T}$ and sound attenuation coefficient $\Gamma_{L,T}$ by

$$\ell_{L,T}(\omega) = \frac{2v_{L,T}}{\Gamma_{L,T}(\omega)} = \frac{2\omega}{k_{L,T}(\omega)\Gamma_{L,T}(\omega)}, \tag{4}$$

If we follow the conventional argumentation of the scaling theory, the states are effectively extended, if the localization length becomes larger than the system size

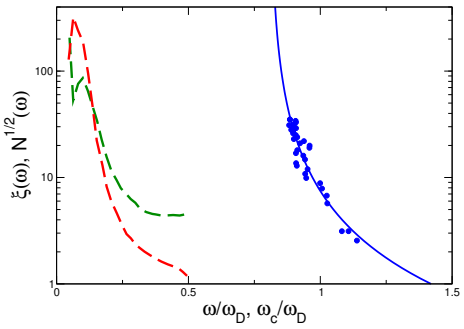

FIG. 4: System size $N^{1/2}$ against the crossover frequency ω_c, divided by the Debye frequency ω_D, (blue symbols), together with the fitting curve (5) and the quantities $\xi_L(\omega)$ and $\xi_T(\omega)$ as determined[77] from our sound attenuation data in Ref.[38]

$N^{1/2}$. If this scenario would hold, $N^{1/2}$ should be related to ω_c by an appropriate combination of the quantities $\xi_{L,T}(\omega_c) \equiv \ell_{L,T}(\omega_c)\exp\{2\omega_c/\Gamma_{L,T}(\omega_c)\}$. In our previous study of the vibrational properties of our model glass[38] we have determined precisely the sound velocities and attenuation coeffients of the longitudinal and transverse vibrational excitations. In Fig. 4 we have plotted the quantities $\xi_{L,T}(\omega_c)$ together with the function $N^{1/2}(\omega_c)$, determined by our study of the size dependence[77]. It is clearly seen that the scaling scenario predicts the crossover in a much lower frequency regime than observed by us. As alternative we have now fitted the crossover frequency with the ansatz

$$\omega_c/\omega_D = aN^{-b} + c, \tag{5}$$

from which we obtained a good fitting result with $a = 0.6 \pm 0.07$, $b = 0.3 \pm 0.1$ and $c = 0.8 \pm 0.05$, given by the curve through the data in Fig. 4. Equation (5) can be inverted to

$$N^{1/2} \propto \xi \propto \left[\frac{\omega_c}{\omega_D} - c\right]^{-\nu} \tag{6}$$

with $\nu = \frac{1}{2b} = 1.66 \pm 0.5$.

We now turn to the question, why should the conventional theory not hold for our model material?

First, let us recall that the orthogonal symmetry class, which gives rise to the one-parameter scaling of the conventional localization theory[74], is only one among 10 possible classes in disordered systems[78,79], where the other classes do not share the property that in two dimensions there is always localization.

The fundamental difference between our model material and many of the model systems studied previously[13,15], is that the disorder does not enter as a prefactor of the time derivative (mass disorder), but as the force constants, which are the off-diagonal matrix elements of the Hessian. This is similar to electronic two-dimensional models, studied recently numerically[53–55], in which the disorder enters via the tight-binding hopping integrals (off-dimensional disorder, "quantum percolation"). In these systems a true metal-nonmetal transition is found, contrary to the prediction of one-parameter scaling[2,11,12]. Our classical system is analogous to the off-diagonal electronic system, whith the difference that in our system the diagonal and off-diagonal matrix elements are related by the stability condition $\sum_j \mathcal{H}_{ij} = 0$. However, a common feature might be that the quantum-interference mechanism, which gives rise to the rigorous localization property in two dimension, might be suppressed by off-diagonal disorder. Here further theoretical work is needed.

One of the nice things with the present experiment is that the spatial distributions of polarization vectors of modes can be directly visualized. Looking at the mode patterns of Fig. 5 the salient features of the vibrational states in the boson-peak and the Debye-frequency frequency regime are visualized. The states in the lower-frequency regime are *delocalized* and show the characteristic eddy pattern of non-affine displacements, which are induced by the structural disorder[80,81]. The states in the boson-peak regime have been classified as "random-matrix states" due to their spectral statistics[82] and "diffusons", because their intensity obey a diffusion equation such as scattered light in milky glass[83]. Another aspect of the boson-peak states is that they abundantly appear in simulations of soft-sphere systems just above the jamming transition[42,57]. In these harmonic and Hertzian models the disorder-induced boson-peak anomaly disappears with increasing the pressure. This is not the case in systems with harder repulsion like ours and like molecular matter. In these systems the disorder is not smoothed out due to the residual structural frustation, which remains, because the repulsive forces inhibit the possiblility of relaxation.

The states near and above the Debye frequency are completely different. They are very much *localized* and have therefore a fundamentally different character as zone-boundary states in crystalline lattices. The latter are also non-propagating, because the oscillating atoms vibrate against each other, but they are *extended*, i.e. they cover the whole crystal. The localized states of disordered materials above the Debye frequency have been shown to form a Lifshitz-type band tail[84,85], as can be seen from Figs. 2 and 3. These states are evanescent defect states, which exist beyond the band edge of the corresponding crystalline lattice. Similar states have been observed recently in a disordered two-dimensional photonic crystal[86] inside the photonic-crystal gap.

In summary, we have performed the first experimental study of level-distance statistics of normal-mode vibrations in densely packed two-dimensional packings of isotropically jammed photoelastic disks. We observe wave delocalization for frequencies smaller than $\omega_c = 0.88 \pm 0.03\omega_D$. Our finite-size study is not compatible with the conventional scaling theory of localization, which states that in two dimension all states are localizes and only predicts a crossover to delocalization if the system size is larger than the localization length. Instead, we obtain a mobility edge in the thermodynamic limit at $\omega_c = 0.8 \pm 0.5\omega_D$. We argue that one-parameter scaling theory might not be applicable to force-constant and off-diagonal disorder.

Our results are surprisingly similar to the situation in three

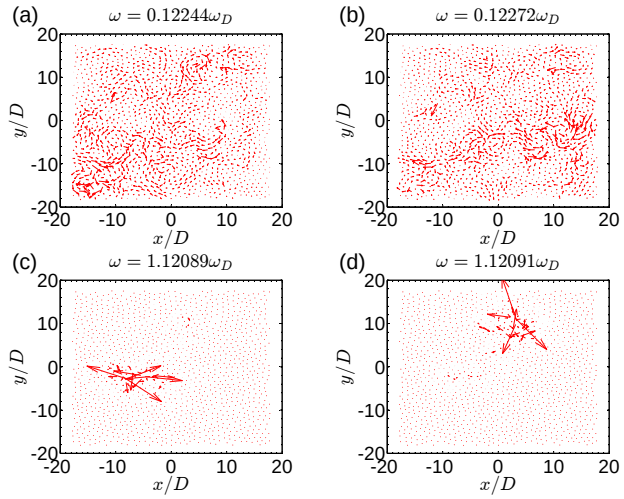

FIG. 5: Comparison between spatial distributions of the modes within the Boson peak (a-b) and Anderson-localization regime (c-d). Here results are shown for a typical value of pressure p = 26.5 N/m, and results of other pressure are similar.

dimensions[22,48–50]: delocalized modes near and above the boson peak and a mobility edge just below the Debye frequency leading to Anderson localization only at the upper end of the band of vibrational modes.

This work is supported by the National Natural Science Foundation of China under (No.11774221 and No. 11974238).

†equal contributions. *(jiezhang2012@sjtu.edu.cn)

[1] P. W. Anderson, Phys. Rev. **109**, 1492 (1958).
[2] E. Abrahams, P. W. Anderson, D. C. Licciardello, and T. V. Ramakrishnan, Phys. Rev. Lett. **42**, 673 (1979).
[3] J. Billy, V. Josse, Z. Zuo, A. Bernard, B. Hambrecht, P. Lugan, D. Clement, L. Sanchez-Palencia, P. Bouyer, and A. Aspect, Nature **453**, 891 (2008).
[4] G. Roati, C. D'Errico, L. Fallani, M. Fattori, C. Fort, M. Zaccanti, G. Modugno, M. Modugno, and M. Inguscio, Nature **453**, 895 (2008).
[5] S. S. Kondov and B. Demarco, Science **334**, 66 (2011).
[6] M. Schreiber, S. S. Hodgman, P. Bordia, H. P. Lüschen, M. H. Fischer, R. Vosk, E. Altman, U. Schneider, and I. Bloch, Science **349**, 842 (2015).
[7] A. A. Chabanov, M. Stoytchev, and A. Z. Genack, Nature **404**, 850 (2000).
[8] T. Schwartz, G. Bartal, S. Fishman, and M. Segev, Nature **446**, 52 (2007).
[9] H. Hu, A. Strybulevych, J. H. Page, S. E. Skipetrov, and B. A. van Tiggelen, Nat. Phys. **4**, 945 (2008).
[10] W. Schirmacher, B. Abaie, A. Mafi, G. Ruocco, and M. Leonetti, Phys. Rev. Lett. **120**, 067401 (2018).
[11] P. A. Lee and T. Ramakrishnan, Reviews of Modern Physics **57**, 287 (1985).
[12] D. Vollhardt and P. Wölfle, Phys. Rev. Lett. **48**, 699 (1982).
[13] S. John, H. Sompolinsky, and M. J. Stephen, Physical Review B **27**, 5592 (1983).
[14] T. R. Kirkpatrick, Phys. Rev. B **31**, 5746 (1985).
[15] C. Monthus and T. Garel, Phys. Rev. B **81**, 224208 (2010).
[16] E. N. Economou, C. M. Soukoulis, and A. D. Zdetsis, Phys. Rev. B **30**, 1686 (1984).
[17] E. Akkermans and R. Maynard, Phys. Rev. B **32**, 7850 (1985).
[18] P. B. Allen and J. L. Feldman, Phys. Rev. Lett. **62**, 645 (1989).
[19] P. B. Allen and J. L. Feldman, Phys. Rev. B **48**, 12581 (1993).
[20] J. J. Freeman and A. C. Anderson, Phys. Rev. B **34**, 5684 (1986).
[21] C. Yu and A. Leggett, Comments on Conden. Matter Phys. **14**, 231 (1988).
[22] W. Schirmacher, G. Diezemann, and C. Ganter, Phys. Rev. Lett. **81**, 136 (1998).
[23] S. N. Taraskin, Y. L. Loh, G. Natarajan, and S. R. Elliott, Phys. Rev. Lett. **86**, 1255 (2001).
[24] W. Schirmacher, Phys. Stat. Sol. (b) **250**, 937 (2013).
[25] M. Baggioli, R. Milkus, and A. Zaccone, Phys. Rev. E **100**, 062131 (2019).
[26] M. Baggioli and A. Zaccone, Phys. Rev. Lett. **122**, 145501 (2019).
[27] L. E. Silbert, A. J. Liu, and S. R. Nagel, Phys. Rev. Lett. **95**, 098301 (2005).
[28] H. Shintani and H. Tanaka, Nat. Mater. **7**, 870 (2008).
[29] G. Monaco and S. Mossa, PNAS **106**, 16907 (2009).
[30] A. Marruzzo, W. Schirmacher, A. Fratalocchi, and G. Ruocco, Sci. Rep. **3**, 1142 (2013).
[31] H. Mizuno, H. Shiba, and A. Ikeda, PNAS **114**, 9767 (2017).
[32] U. Buchenau, M. Prager, N. Nücker, A. J. Dianoux, N. Ahmad, and W. A. Phillips, Phys. Rev. B **34**, 5665 (1986).
[33] V. K. Malinovsky and A. P. Sokolov, Sol. State Commun. **57**, 757 (1986).
[34] C. Brito, O. Dauchot, G. Biroli, and J. P. Bouchaud, Soft Matter **6**, 3013 (2010).
[35] A. I. Chumakov, G. Monaco, A. Monaco, W. A. Crichton, A. Bosak, R. Rüffer, A. Meyer, F. Kargl, L. Comez, D. Fioretto, et al., Phys. Rev. Lett. **106**, 225501 (2011).
[36] A. I. Chumakov, G. Monaco, A. Fontana, A. Bosak, R. P. Hermann, D. Bessas, B. Wehinger, W. A. Crichton, M. Krisch, and R. Rüffer, Phys. Rev. Lett. **112**, 339 (2014).
[37] L. Zhang, J. Zheng, Y. Wang, L. Zhang, Z. Jin, L. Hong, Y. Wang, and J. Zhang, Nat. Commun. **8**, 67 (2017).
[38] Y. Wang, L. Hong, Y. Wang, W. Schirmacher, and J. Zhang, Phys. Rev. B **98**, 174207 (2018).
[39] X. Li, H. Zhang, S. Lan, D. L. Abernathy, T. Otomo, F. Wang, Y. Ren, M. Li, and X.-L. Wang, Physical Review Letters **124**, 225902 (2020).
[40] P. Sheng, M. Zhou, and Z. Q. Zhang, Phys. Rev. Lett. **72**, 234 (1994).
[41] W. Schirmacher and G. Diezemann, Ann. Phys. **49**, 727 (1999).
[42] C. S. O'Hern, L. E. Silbert, A. J. Liu, and S. R. Nagel, Phys. Rev. E **68**, 011306 (2003).
[43] E. Degiuli, A. Laversanne-Finot, G. Düring, E. Lerner, and M. Wyart, Soft Matter **10**, 5628 (2014).
[44] S. Franz, G. Parisi, P. Urbani, and F. Zamponi, PNAS **112**, 14539 (2015).
[45] P. Charbonneau, E. I. Corwin, G. Parisi, A. Poncet, and F. Zamponi, Phys. Rev. Lett. **117**, 045503 (2016).
[46] K. Chen, M. L. Manning, P. J. Yunker, W. G. Ellenbroek, Z. Zhang, A. J. Liu, and A. G. Yodh, Phys. Rev. Lett. **107**, 108301 (2011).
[47] F. M. Izrailev, Physics Reports **196**, 300 (1990).
[48] W. Schirmacher and M. Wagener, Sol. State Commun. **86**, 597 (1993).
[49] S. D. Pinski, W. Schirmacher, and R. A. Römer, Europhys. Lett. **97**, 16007 (2012).

[50] S. D. Pinski, W. Schirmacher, T. Whall, and R. A. Römer, J. Phys.: Condens. Matter **24**, 405401 (2012).

[51] B. J. Huang and T. M. Wu, Phys. Rev. E **79**, 041105 (2009).

[52] $\omega_D = v_D k_D$ is the Debye frequency, with the Debye velocity $v_D^{-1} = \frac{1}{2}[v_L^{-1} + v_T^{-1}]$ and the Debye wavenumber $k_D = \sqrt{4\pi N/A}$. $v_{L,T}$ are the longitudinal and transverse sound velocities, obtained from the wavenumber dependent velocity correlation functions[38], N is the number of disks, and A is the sample area.

[53] M. F. Islam and H. Nakanishi, Phys. Rev. E **77**, 061109 (2008).

[54] B. S. Dillon Thomas and H. Nakanishi, Eur. Phys. J. B **94**, 286 (2014).

[55] B. S. Dillon Thomas and H. Nakanishi, Phys. Rev. E **94**, 042141 (2016).

[56] This protocol has been shown recently to be equivalent to simulations of colloidal packings prepared by frictionless compression, see A. Lemaître *et al.* arXiv:2008.12917 and arXiv:2010.03239.

[57] M. Wyart, L. E. Silbert, S. R. Nagel, and T. A. Witten, Phys. Rev. E **72**, 051306 (2005).

[58] The material of our disks has a bulk modulus of $B = 4$ MPa, which gives a microscopic pressure per disk of $p\mathsf{mic} = BD/2 = 24 \cdot 10^3$ N/m. This gives for a typical value of our applied pressure $p = 26.5$ N/m a relative pressure of $p_{\mathsf{rel}} = p/p_{\mathsf{mic}} \approx 0.001$. Values of this ratio near the jamming point in the soft-sphere simulations[42] are in the range below $\approx 10^{-6}$. This shows that with our pressure conditions we are at least three orders of magnitude above the jamming limit.

[59] While we are just recording the dynamical matrix of our system statically, we are able to reconstruct the complete vibrational spectrum[37,38].

[60] C. E. Maloney and A. Lemaitre, Phys. Rev. E **74**, 016118 (2006).

[61] W. G. Ellenbroek, M. van Hecke, and W. van Saarloos, Phys. Rev. E **80**, 061307 (2009).

[62] E. Degiuli, E. Lerner, C. Brito, and M. Wyart, PNAS **111**, 17054 (2014).

[63] M. L. Mehta, Random matrices (Academic Press, San Diego, USA, 1991).

[64] H.-J. Stöckmann, Quantum chaos (Cambridge University Press, Cambridge, UK, 1999).

[65] S. N. Evangelou, Phys. Rev. B **49**, 16805 (1994).

[66] I. Zharekeshev and B. Kramer, Phys. Rev. Lett. **79**, 717 (1997).

[67] P. Carpena and P. Bernaola-Galván, Phys. Rev. B **60**, 201 (1999).

[68] S. Sastry, N. Deo, and S. Franz, Phys. Rev. E **64**, 016305 (2001).

[69] S. Ciliberti and T. S. Grigera, Phys. Rev. E **70**, 061502 (2004).

[70] M. Serbyn and J. E. Moore, Phys. Rev. B **93** (2016).

[71] D. Vollhardt and P. Wölfle, Phys. Rev. Lett. **45**, 842 (1980).

[72] D. Vollhardt and P. Wölfle, Phys. Rev. B **22**, 4666 (1980).

[73] P. Wölfle and D. Vollhardt, Int. J. Mod. Phys. B **24**, 1526 (2010).

[74] F. Wegner, Z. Phys. B **35**, 207 (1979).

[75] L. Schäfer and F. Wegner, Z. Phys. B **38**, 113 (1980).

[76] A. J. McKane and M. Stone, Ann. Phys. (N. Y.) **131**, 36 (1981).

[77] For the coefficient in the exponent of Eq. 3 we have taken $C = 1$. For values of C differing from 1 the curves would be slightly shifted upwards or downwards, but not to the right.

[78] A. Altland and M. R. Zirnbauer, Phys. Rev. B **55**, 1142 (1997).

[79] F. Evers and A. D. Mirlin, Rev. Mod. Phys. **80**, 1355 (2008).

[80] A. Lemaître and C. Malonay, J. Stat. Phys. **123**, 415 (2006).

[81] F. Léonforte, A. Tanguy, J. P. Wittmer, and J.-L. Barrat, Phys. Rev. Lett. **97**, 055501 (2006).

[82] W. Schirmacher, T. Scopigno, and G. Ruocco, J. Noncryst. Sol. **407**, 133 (2015).

[83] P. B. Allen, J. L. Feldman, J. Fabian, and F. Wooten, Phys. Rev. B **48**, 12589 (1999).

[84] I. Lifshitz, Adv. Phys. **46**, 483 (1964).

[85] C. Tomaras and W. Schirmacher, J. Phys. Condens. Matter **25**, 495402 (2013).

[86] J. M. Escalante and S. E. Skipetrov, Sci. Rep. **8**, 11569 (2018).